CROMER, D. T. & WABER, J. T. (1965). *Acta Cryst.* **18**, 104–109.
CRUICKSHANK, D. W. J., PILLING, D. E., BUJOSA, A., LOVELL, F. M. & TRUTER, M. R. (1961). *Computing Methods and the Phase Problem in X-ray Crystal Analysis*. Oxford: Pergamon Press.
DIVJAKOVIĆ, V. & NOWACKI, W. (1975). *Z. Kristallogr.* **142**, 262–270.
EDENHARTER, A. (1976). *Schweiz. Mineral. Petrogr. Mitt.* **56**, 195–217.
HERBERT, H. K. & MUMME, W. G. (1980). *Neues Jahrb. Mineral. Monatsh.* In the press.
KALBSKOPF, R. (1971). *Tschermaks Mineral. Petrogr. Mitt.* **16**, 173–175.
MAKOVICKY, E. & MUMME, W. G. (1979). *Can. Mineral.* **17**, 607–618.
MAKOVICKY, E., MUMME, W. G. & WATTS, J. A. (1977). *Can. Mineral.* **15**, 339–348.
MULLEN, D. J. E. (1974). *Z. Kristallogr.* **140**, 27–49.
NIIZEKI, W. & BUERGER, M. J. (1957). *Z. Kristallogr.* **109**, 129–157.
OHMASA, M. (1973). *Neues Jahrb. Mineral. Monatsh.* pp. 227–233.
OHMASA, M. & NOWACKI, W. (1971). *Z. Kristallogr.* **134**, 360–380.
OHMASA, M. & NOWACKI, W. (1973). *Z. Kristallogr.* **137**, 422–432.
SRIKRISHNAN, T. & NOWACKI, W. (1975). *Z. Kristallogr.* **141**, 174–192.
TAKEUCHI, Y., TAKAGI, J. & YAMANAKA, T. (1974). *Proc. Jpn Acad.* **50**, 317–321.

Acta Cryst. (1980). B**36**, 1304–1311

The Structure of Mooreite

BY RODERICK J. HILL

CSIRO Division of Mineral Chemistry, PO Box 124, *Port Melbourne, Victoria, Australia* 3207

(*Received* 17 *September* 1979; *accepted* 12 *February* 1980)

Abstract

Mooreite, $Mg_{9.10}Zn_{4.04}Mn_{1.89}(SO_4)_2(OH)_{26}.8H_2O$, from Sterling Hill, New Jersey, crystallizes in space group $P2_1/a$ with $a = 11.147$ (3), $b = 20.350$ (6), $c = 8.202$ (3) Å, $\beta = 92.69$ (4)°, and $Z = 2$. The crystal structure has been determined by Patterson and Fourier methods from 3276 graphite-monochromatized Mo $K\alpha$ data and refined by least-squares methods (including the H atoms) to an R value of 0·066 ($R_w = 0.028$). The fundamental building units of the structure are brucite-like sheets of edge-sharing Mg octahedra, with ideal composition $[Mg_{4.5}(OH)_{11}]^{2-}$, oriented parallel to (010) and separated by $\frac{1}{2}b$. The vacant octahedral sites in these sheets share their upper and lower faces with tetrahedral $[Zn(OH)_4]^{2-}$ groups, each projecting a vertex into the interlayer region. Tetrahedron vertices from opposite sides of adjacent sheets are in turn shared (in a *cis* relationship) with otherwise insular $Mn(OH)_2(H_2O)_4$ octahedra sandwiched between the sheets. Aside from several rather weak hydrogen bonds between the hydroxyl groups and water molecules, the corner-sharing between Zn tetrahedra and Mn octahedra is the only connection between the brucite layers, thereby accounting for the perfect {010} cleavage and platy habit of the mineral. The sulphate groups occupy large cavities between the Mn octahedra in the interlayer region and are held rather loosely in position by hydrogen bonding alone. Up to 12% of the cations are disordered over the octahedral sites in both the brucite and Mn layers, but this has no significant effect on the polyhedron bond lengths.

0567-7408/80/061304-08$01.00

Introduction

The rare mineral mooreite, previously $(Mg,Zn,Mn)_8(SO_4)(OH)_{14}.3$–$4H_2O$ with $Z = 4$, occurs as transparent, tabular crystals in cavities and veinlets in massive calcite–franklinite–willemite ore at Sterling Hill, New Jersey (Bauer & Berman, 1929). Subsequent studies by Prewitt-Hopkins (1949) and Finney (1969) concentrated on chemical and physical properties of the mineral, but disagree on the unit-cell dimensions and symmetry, and also on the number of water molecules in the structural formula. Using a new set of chemical data and preliminary results from the present crystal structure analysis Hill (1979) determined that there are only 7·5 cations in the asymmetric unit and proposed the new formula $Mg_{9.10}Zn_{4.04}Mn_{1.89}(SO_4)_2(OH)_{26}.8H_2O$ with $Z = 2$. Information was also provided on the unit-cell dimensions and space-group symmetry (included in the *Abstract*), along with the X-ray diffraction pattern and infrared absorption spectrum. The detailed results of the crystal structure analysis are presented herein. Material for the in-

vestigation was kindly made available by Dr C. A. Francis of the Harvard Mineralogical Museum (specimen No. 90395).

Experimental

The crystal selected for data collection was a transparent, essentially equidimensional pentagonal prism with mean edge length 0·062 mm and thickness 0·075 mm. The specimen was mounted on a Philips PW 1100 four-circle automatic diffractometer in an arbitrary orientation and intensity data were collected at 295 K with Mo $K\alpha$ radiation monochromatized by a flat graphite crystal (λ = 0·7093 Å; $2\theta_m$ = 12·0°) using a θ–2θ scan technique and a 2θ scan rate of 2° min^{-1}. Backgrounds were determined from 10 s stationary counts at both ends of each dispersion-corrected (Alexander & Smith, 1964) scan range (minimum width = 1·1° in 2θ). Three non-coplanar reflections measured every two hours showed no significant variations in either intensity or position. A total of 11 749 reflections were collected from the positive l hemisphere to a maximum 2θ value of 65° and the resultant data were corrected for background, Lorentz and polarization effects using a program written specifically for the PW 1100 diffractometer by Hornstra & Stubbe (1972). Since the plane of reflection of the graphite monochromator was perpendicular to that of the specimen crystal, the Lorentz–polarization correction was of the form $Lp^{-1} = \sin 2\theta(1 + \cos^2 2\theta_m)/(\cos^2 2\theta + \cos^2 2\theta_m)$, where θ_m is the Bragg angle of the monochromator. Absorption corrections were then applied to the data with the Gaussian quadrature method as coded in the *SHELX* system of programs (Sheldrick, 1976) using a 2 × 2 × 5 grid and a μ value of 3·62 mm^{-1}: the minimum and maximum transmission factors were 0·721 and 0·787 respectively. Multiply measured and symmetry-equivalent reflections consistent with point group $2/m$ were then averaged to yield a set of 5726 unique structure factors, F, each with a standard deviation estimated from the equation $\sigma_F = [\sigma_I^2 + (0{\cdot}03I)^2]^{0{\cdot}5}/2I^{0{\cdot}5}$, where I is the corrected raw intensity and σ_I is derived from counting and averaging statistics. The overall agreement factor between averaged intensities was 0·074, but only those 3276 observations with $F > 3\sigma_F$ were included in the subsequent least-squares analysis.

Structure determination and refinement

A single Zn atom [Zn(1) in Table 1] was located from the Patterson function and the remaining Zn, Mn, S, 5 Mg and 21 O atoms in the asymmetric unit from successive partially phased Fourier syntheses. The coordinates and isotropic temperature factors of these atoms were refined in space group $P2_1/a$ by least-squares minimization of the function $\sum w(|F_o| - |F_c|)^2$, where F_o and F_c are the observed and calculated structure factors, and $w = 1/\sigma_F^2$, to yield a conventional R_w value of 0·064. At this stage it was observed that the temperature factors of all five Mg atoms were somewhat smaller (B = 0·13 to 0·55 Å^2), and that of the Mn atom somewhat larger (B = 1·52 Å^2) than expected for octahedrally coordinated cations. The population parameters for these atoms were therefore released in all subsequent refinements in a

Table 1. *Fractional atomic coordinates*

Population parameters for Zn atoms were set to 1·0 in the final cycles.

		x	y	z	Population parameters
Zn(1)		0.23039(6)	0.08363(3)	0.90475(7)	0.995(2)
Zn(2)		0.27372(6)	0.40940(3)	0.09073(7)	0.993(2)
Mg(1)		0.04530(11)	-0.00217(8)	0.18168(14)	1.094(4)
Mg(2)		0.31801(13)	-0.00420(8)	0.27219(16)	1.080(4)
Mg(3)		0.13643(12)	-0.00408(8)	0.54463(15)	1.066(4)
Mg(4)		0.40908(12)	0.00041(9)	0.63507(15)	1.048(5)
Mg(5)		0.5	0.0	0.0	1.117(6)
Mn		0.36743(8)	0.24605(4)	0.98358(9)	0.941(2)
S		0.12580(14)	0.22529(6)	0.46938(17)	
O(1)		0.0342(5)	0.1808(2)	0.4090(7)	
O(2)		0.2400(4)	0.1926(2)	0.4612(5)	
O(3)		0.1166(4)	0.2836(2)	0.3681(5)	
O(4)		0.1074(6)	0.2396(3)	0.6325(4)	
O(5)	OH	0.2452(4)	0.3146(2)	0.0768(4)	
O(6)	OH	0.2286(5)	0.1808(2)	0.9099(4)	
O(7)	OH	0.1676(3)	0.0463(1)	0.3298(4)	
O(8)	OH	0.4379(3)	0.0504(1)	0.4213(4)	
O(9)	OH	-0.0109(3)	0.0510(1)	0.6069(4)	
O(10)	OH	0.0718(4)	0.0542(2)	-0.0293(5)	
O(11)	OH	0.2580(3)	0.0567(1)	0.6803(4)	
O(12)	OH	0.3527(3)	0.0559(2)	0.0670(4)	
O(13)	OH	0.1170(3)	0.4423(2)	0.1552(5)	
O(14)	OH	0.2109(3)	0.4462(1)	0.5130(4)	
O(15)	OH	0.3067(3)	0.4380(2)	0.8691(4)	
O(16)	OH	0.4008(3)	0.4393(1)	0.2469(4)	
O(17)	OH	0.0277(3)	0.4503(1)	0.7907(4)	
O(18)	H_2O	0.0174(4)	0.1877(2)	0.0606(4)	
O(19)	H_2O	0.3987(4)	0.1903(2)	0.2153(5)	
O(20)	H_2O	0.0287(4)	0.3110(2)	0.8884(4)	
O(21)	H_2O	0.3602(4)	0.2956(2)	0.7405(5)	
H(5)		0.231(6)	0.307(3)	0.153(6)	
H(6)		0.214(7)	0.187(4)	0.857(8)	
H(7)		0.171(6)	0.082(2)	0.341(7)	
H(8)		0.450(6)	0.085(2)	0.426(7)	
H(9)		0.000(6)	0.084(2)	0.599(7)	
H(10)		0.057(6)	0.078(3)	-0.004(8)	
H(11)		0.259(5)	0.092(2)	0.640(6)	
H(12)		0.375(6)	0.083(3)	0.105(7)	
H(13)		0.085(6)	0.418(3)	0.164(8)	
H(14)		0.224(6)	0.414(2)	0.500(7)	
H(15)		0.316(6)	0.403(2)	0.818(6)	
H(16)		0.431(5)	0.406(2)	0.287(6)	
H(17)		0.030(5)	0.409(2)	0.800(6)	
H(181)		0.025(7)	0.199(3)	0.128(7)	
H(186)		0.097(5)	0.180(2)	0.003(6)	
H(192)		0.355(5)	0.189(3)	0.302(6)	
H(193)		0.442(6)	0.204(3)	0.243(8)	
H(204)		0.032(5)	0.298(3)	0.792(6)	
H(205)		0.084(5)	0.316(3)	0.970(6)	
H(214)		0.404(6)	0.292(3)	0.687(8)	
H(214')		0.303(5)	0.282(3)	0.685(7)	

crude attempt to account for the inferred presence of cation disorder among the octahedral sites: no such adjustments appeared to be necessary for the tetrahedrally coordinated Zn atoms (confirmed by later site-occupancy refinement) since their isotropic temperature factors were 0·76 and 0·83 Å^2. With the inclusion of the population parameters and an isotropic extinction parameter as defined by Larson (1967) in the refinement the temperature factors all became more reasonable and the R_w value dropped to 0·060.

A Fourier difference synthesis was then computed, utilizing only those data with sin $\theta/\lambda < 0{\cdot}4$ Å^{-1}, and peaks ranging from 0·4 to 0·9 e Å^{-3} were found for all 21 H atoms in the asymmetric unit. There were also a small number of other peaks with maximum density less than 10% of the magnitude of an O atom peak but these were all located well within the coordination spheres of Zn, Mn and Mg or in the immediate vicinity of the rather loosely bound sulphate group. Refinement was then continued with anisotropic temperature factors assigned to all non-H atoms and the H atoms fixed at their difference map positions with isotropic temperature factors of 4·0 Å^2 to yield an R_w value of 0·033. The H-atom coordinates were then released, but the available computer space would not allow all of the resulting 338 variables to be varied simultaneously in full-matrix refinement. The atoms were therefore divided into two blocks, one representing the 29 atoms associated with the 'brucite-like' layers of Mg octahedra and Zn tetrahedra parallel to (010), and the other block incorporating the remaining 22 atoms of the Mn octahedra and sulphate tetrahedra in the interlayer region. Refinement then proceeded smoothly to convergence (parameter shifts in the final cycle were less than one fifth of the appropriate e.s.d.) at R_w and R values of 0·028 and 0·066 respectively. The final value for the extinction parameter was 1·9 (2) $\times 10^{-3}$ and the error in an observation of unit weight was 0·137. Atomic coordinates along with their standard deviations estimated from the inverted matrices are given in Table 1. The r.m.s. components of thermal displacement, and thermal-ellipsoid orientations appear in Table 2.*

Scattering factors for Zn, Mn, Mg, S and O (neutral atoms) were obtained from *International Tables for X-ray Crystallography* (1974) and were corrected for both real and imaginary anomalous-dispersion components. For H, the spherical scattering factor suggested by Stewart, Davidson & Simpson (1965) was used. Structure solution, refinement and geometry calculations were all performed with the XRAY 76 system of programs (Stewart, 1976).

* Lists of structure factors, anisotropic thermal parameters and Table 2 have been deposited with the British Library Lending Division as Supplementary Publication No. SUP 35116 (37 pp.). Copies may be obtained through The Executive Secretary, International Union of Crystallography, 5 Abbey Square, Chester CH1 2HU, England.

Discussion of the structure

Mooreite crystallizes with the topology displayed in Figs. 1, 2 and 3, and the bonding dimensions summarized in Tables 3 and 4.

In summary, the structure consists of brucite-like sheets of edge-sharing $Mg(OH)_6$ octahedra with overall composition $[Mg_{4.5}(OH)_{11}]^{2-}$, oriented parallel to (010) and separated by $\frac{1}{2}b$ (10·2 Å). Vacant octahedral sites in these sheets share their upper and lower faces with tetrahedral $Zn(OH)_4$ groups projecting their fourth vertex into the interlayer region. Zn tetrahedron vertices from opposite sides of adjacent sheets are in turn shared with otherwise isolated $Mn(OH)_2(H_2O)_4$ octahedra sandwiched between the sheets. The sulphate groups occupy rather large cavities between the Mn octahedra in the interlayer region and are held in place by hydrogen bonds from both the hydroxyl groups and water molecules.

To the author's knowledge the mooreite structure type is unique, although the Mg octahedron/Zn tetrahedron layer is similar to the arrangement of octahedra and tetrahedra in $Zn_5(OH)_8Cl_2.H_2O$ (Allmann, 1968), $Zn_5(OH)_6(CO_3)_2$ (hydrozincite; Ghose, 1964), and $Zn_5(OH)_8(NO_3)_2.2H_2O$ (Stahlin & Oswald, 1970). In all four compounds the Zn tetrahedra are located above and below vacant sites in a

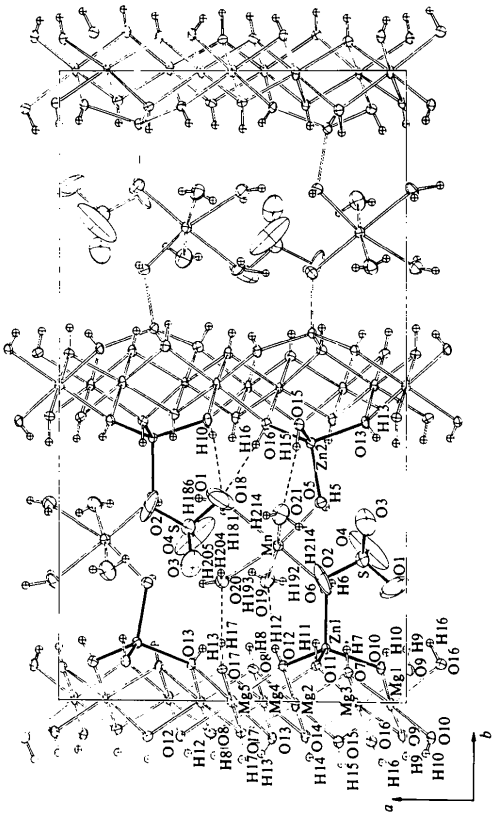

Fig. 1. Unit-cell diagram of the mooreite crystal structure viewed down the *c* axis. Thermal ellipsoids for all atoms (*B* for hydrogen set = 0·5 Å^2) represent 50% probability surfaces. The tetrahedral ZnO_4 and SO_4 groups in the atom-labelled portion of the diagram have been indicated by filled conical bonds, and the hydrogen bonds by dashed lines.

Table 3. *Interatomic distances* (Å) *and angles* (°) *involving the nonhydrogen atoms*

Zn(1) tetrahedron

Zn(1)-O(12)	1.943(4)	O(12)-O(11)	3.295(5)	115.2(1)
O(11)	1.959(3)	O(10)	3.193(6)	109.5(2)
O(10)	1.966(4)	O(6)	3.142(6)	106.5(2)
O(6)	1.978(5)	O(11)-O(10)	3.232(5)	110.9(1)
average =	1.962	O(6)	3.177(5)	107.6(1)
		O(10)-O(6)	3.166(6)	106.8(2)

Zn(2) tetrahedron

Zn(2)-O(5)	1.957(4)	O(5)-O(15)	3.129(5)	106.0(1)
O(15)	1.961(3)	O(16)	3.342(5)	117.0(1)
O(16)	1.962(3)	O(13)	3.048(5)	101.9(2)
O(13)	1.966(4)	O(15)-O(16)	3.225(5)	110.6(1)
average =	1.962	O(13)	3.233(5)	110.9(2)
		O(16)-O(13)	3.218(5)	110.0(1)

S tetrahedron

S-O(4)	1.394(4)	O(4)-O(1)	2.306(7)	109.2(4)
O(1)	1.435(5)	O(2)	2.295(7)	108.1(3)
O(2)	1.441(5)	O(3)	2.353(6)	111.7(3)
O(3)	1.449(4)	O(1)-O(2)	2.326(7)	108.0(3)
average =	1.430	O(3)	2.315(6)	106.8(3)
		O(2)-O(3)	2.409(6)	112.9(3)

Mn octahedron

Mn-O(6)	2.106(5)	O(6)-O(5)	3.050(6)	92.4(2)
O(5)	2.118(4)	O(19)	3.076(6)	90.4(2)
O(18)	2.217(5)	O(21)	3.119(7)	91.9(2)
O(19)	2.227(4)	O(20)	3.363(7)	99.2(2)
O(21)	2.232(4)	O(5)-O(18)	3.044(6)	89.2(2)
O(20)	2.307(4)	O(19)	3.232(6)	96.0(1)
average =	2.201	O(21)	3.120(6)	91.6(2)
		O(18)-O(19)	3.113(6)	88.9(2)
		O(21)	3.106(6)	88.5(2)
		O(20)	2.885(6)	79.2(2)
		O(19)-O(20)	3.107(6)	86.5(1)
		O(21)-O(20)	3.081(6)	85.5(2)

Mg(1) octahedron

Mg(1)-O(7)	2.037(4)	O(7)-O(9) S	2.707(5)	82.9(1)
O(9)	2.051(4)	O(15) S	2.763(4)	83.6(1)
O(10)	2.058(4)	O(10)'	3.089(5)	96.3(2)
O(15)	2.107(4)	O(16)	3.033(5)	93.0(1)
O(10)'	2.108(4)	O(9)-O(15)	3.036(5)	93.8(1)
O(16)	2.144(4)	O(10)	3.082(5)	97.2(2)
average =	2.084	O(16) S	2.824(5)	84.6(1)
		O(10)'-O(10) S	2.781(5)	83.7(2)
		O(15)	2.997(5)	90.6(1)
		O(16)	3.031(5)	90.9(1)
		O(15)-O(10)	3.036(6)	93.6(2)
		O(10)-O(16)	2.966(5)	89.8(1)

Mg(2) octahedron

Mg(2)-O(7)	2.041(4)	O(7)-O(14) S	2.735(5)	83.4(1)
O(17)	2.041(4)	O(8)	3.072(5)	96.1(1)
O(14)	2.069(4)	O(15) S	2.763(4)	83.2(1)
O(8)	2.089(4)	O(12)	3.060(5)	94.3(1)
O(15)	2.123(4)	O(17)-O(14)	3.131(5)	99.2(1)
O(12)	2.130(4)	O(8) S	2.718(4)	82.3(1)
average =	2.082	O(15)	3.156(5)	98.6(1)
		O(12) S	2.759(5)	82.8(1)
		O(14)-O(8) S	2.761(5)	83.2(1)
		O(15)	3.067(5)	94.1(1)
		O(8)-O(12)	3.017(5)	91.3(1)
		O(15)-O(12)	3.045(5)	91.4(1)

Mg(3) octahedron

Mg(3)-O(14)	2.054(4)	O(14)-O(9)	3.161(5)	100.3(2)
O(9)	2.063(4)	O(7) S	2.735(5)	82.8(1)
O(9)	2.072(4)	O(11) S	2.782(5)	83.8(1)
O(7)	2.081(4)	O(16)	3.115(5)	96.5(1)
O(11)	2.112(4)	O(9)-O(9) S	2.737(5)	82.9(1)
O(16)	2.119(4)	O(7)	3.092(5)	96.2(1)
average =	2.084	O(11)	3.031(5)	92.8(1)
		O(16) S	2.824(5)	84.7(1)
		O(7)-O(9) S	2.707(5)	81.6(1)
		O(11)	3.009(5)	91.7(1)
		O(11)-O(16)	3.049(5)	92.2(1)
		O(16)-O(9)	3.075(5)	94.7(1)

Mg(4) octahedron

Mg(4)-O(17)	2.056(4)	O(17)-O(8)	3.146(5)	99.5(1)
O(8)	2.066(4)	O(8)' S	2.718(4)	82.5(1)
O(8)'	2.066(4)	O(11)	3.102(5)	97.0(1)
O(14)	2.080(4)	O(13) S	2.765(5)	83.0(1)
O(11)	2.084(4)	O(8)-O(8)' S	2.763(5)	83.9(1)
O(13)	2.119(4)	O(14) S	2.761(5)	83.5(1)
average =	2.079	O(11)	2.992(5)	92.3(1)
		O(14)-O(8)'	3.101(5)	96.8(1)
		O(11) S	2.782(5)	83.8(1)
		O(13)	3.070(5)	94.0(1)
		O(11)-O(13)	3.001(5)	91.1(1)
		O(13)-O(8)'	3.030(5)	92.8(1)

Mg(5) octahedron

Mg(5)-O(17)×2	2.029(3)	O(17)-O(12)×2	3.061(5)	95.9(1)
O(12)×2	2.092(4)	O(12)×2 S	2.759(5)	84.1(1)
O(13)×2	2.132(4)	O(13)×2	3.111(5)	96.7(1)
average =	2.084	O(13)×2 S	2.765(5)	83.3(1)
		O(12)-O(13)×2	3.001(5)	90.5(1)
		O(13)×2	2.973(5)	89.5(1)

Shared edges between occupied octahedra are indicated by S

CdI_2 (brucite)-type sheet of Mg or Zn octahedra, but differ in the manner in which the remaining groups are incorporated between the layers. In $Zn_5(OH)_8Cl_2.H_2O$ the chloride ion is directly coordinated to the tetrahedral Zn atom and the water molecule occupies disordered positions between the sheets; in hydrozincite the carbonate group coordinates both the octahedral and tetrahedral Zn atoms across the interlayer region; in $Zn_5(OH)_8(NO_3)_2.2H_2O$ the water molecules are coordinated to the tetrahedral Zn atom but the nitrate groups are held in place only by hydrogen bonds from adjacent sheets.

The magnesium octahedron layer

The layer of edge-sharing $Mg(OH)_6$ octahedra is seen 'edge-on' in Fig. 1, and from above in Fig. 2. The hydroxyl groups occur in positions of approximate hexagonal close packing and the Mg atoms occupy all but one of the available octahedral interstices, resulting in an overall sheet composition of $[Mg_{4.5}(OH)_{11}]^{2-}$. With the exception of the missing Mg atom this unit bears a striking resemblance to the $Mg(OH)_2$ layers in brucite (Aminoff, 1921; Zigan & Rothbauer, 1967). In both structures the O—H bonds are oriented perpendicular to the sheets (Figs. 1 and 2) and, insofar as the shared edges of each octahedron are shorter than the unshared ones, the sheets are considerably flattened. In brucite the sheets have a uniform thickness of 2·112 Å, relative to the undistorted value of 2·427 Å, but in mooreite the situation is complicated by the presence of the vacant octahedral site and the fact that only four or five of the edges of each octahedron are shared. The sheet has a mean thickness of 2·214 Å but varies from

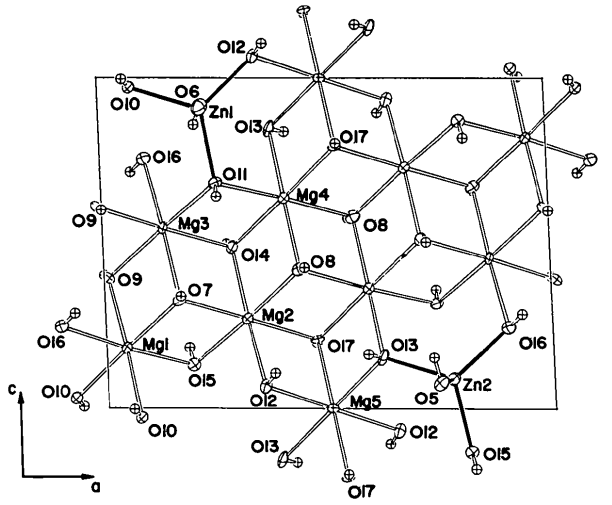

Fig. 2. Diagram of the magnesium octahedron sheet at $y = 0$ in the mooreite unit cell. Two crystallographically independent ZnO_4 tetrahedra attached to the upper surface of the sheet above vacant octahedral sites are indicated by filled conical bonds. Tetrahedra on the lower side, along with H-atom labels, have been omitted for clarity. Thermal ellipsoids are as in Fig. 1.

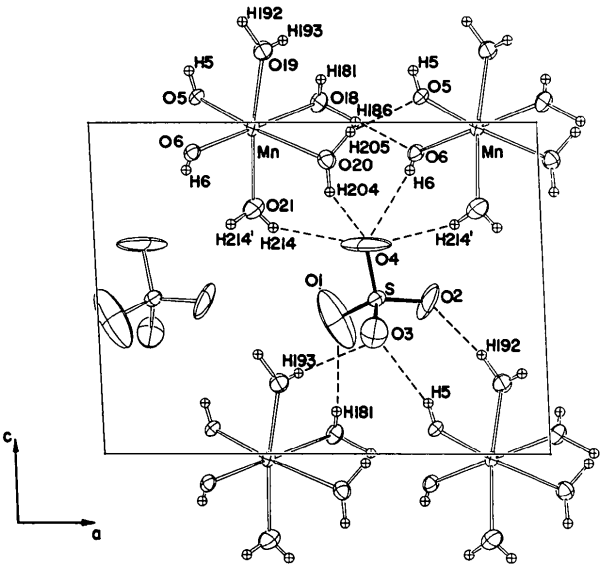

Fig. 3. Diagram of the interlayer region at $y = \frac{1}{4}$ in the mooreite unit cell. The hydrogen and S—O bonds associated with one of the sulphate groups in this layer have been indicated by dashed lines and filled conical bonds respectively. Thermal ellipsoids are as in Fig. 1.

2·045 Å in those areas some distance from the vacant site to a value of 2·355 Å for the vacant octahedron itself. These differences in thickness reflect differences in the degree of shared-edge shortening in the various regions of the sheet: the edges shared between occupied octahedra have lengths in the range 2·707 to 2·824 Å (relative to an undistorted value of 2·946 Å) whereas those shared between occupied and vacant octahedra have lengths from 2·966 to 3·049 Å (the shared edges

Table 4. *Hydrogen-bond distances* (Å) *and angles* (°)

H	O_d	O_a	O_d–H	H···O_a	O_d···O_a	∠O_d–H···O_a	∠H–O_d–H
H(5)	O(5)	O(3)	0.67(5)	2.28(6)	2.912(6)	159(7)	
H(6)	O(6)	O(4)	0.48(6)	2.39(7)	2.853(6)	164(11)	
H(7)	O(7)		0.73(5)				
H(8)	O(8)		0.73(4)				
H(9)	O(9)		0.68(5)				
H(10)	O(10)	O(18)	0.56(6)	2.34(5)	2.886(5)	169(8)	
H(11)	O(11)		0.79(5)				
H(12)	O(12)	O(19)	0.67(5)	2.37(5)	3.027(5)	164(7)	
H(13)	O(13)		0.62(6)				
H(14)	O(14)		0.68(5)				
H(15)	O(15)	O(21)	0.83(5)	2.34(5)	3.151(6)	166(5)	
H(16)	O(16)	O(1)	0.81(5)	2.32(5)	3.125(6)	174(5)	
H(17)	O(17)	O(20)	0.85(4)	2.12(4)	2.946(5)	165(5)	
H(181)	O(18)	O(1)	0.60(6)	2.33(6)	2.858(7)	149(8)	113(8)
H(186)		O(6)	1.03(5)	1.69(5)	2.714(7)	170(4)	
H(192)	O(19)	O(2)	0.88(5)	1.87(5)	2.745(6)	170(5)	100(7)
H(193)		O(3)	0.59(6)	2.17(6)	2.733(6)	159(8)	
H(204)	O(20)	O(4)	0.83(5)	1.98(5)	2.731(6)	149(5)	133(5)
H(205)		O(5)	0.90(5)	1.96(5)	2.804(6)	157(5)	
H(214)	O(21)	O(4)	0.67(6)	2.42(6)	3.020(8)	149(7)	100(7)
H(214')		O(4)	0.82(6)	2.36(6)	3.129(8)	157(6)	

between occupied octahedra are marked with an *S* in Table 3). In fact, there is also a systematic variation in the lengths of the occupied-octahedron shared edges according to whether or not one of the bridging hydroxyl groups forms part of the unoccupied octahedron: in the former case the edges have lengths between 2·707 and 2·763 Å, and in the latter case the range is 2·759 to 2·824 Å. As expected, the unshared edges on the top and bottom of the sheet compensate for the shortening achieved for the shared edges by lengthening to values between 2·992 and 3·161 Å.

Although the maximum variation in Mg—O bond lengths within and between the five Mg octahedra is relatively small (0·115 Å), there is a uniform tendency for the bonds to the O atoms of the unoccupied octahedron to be slightly longer (by 0·053 Å) than those to O atoms involved only in the occupied octahedra. This is to be expected from electrostatic bond-strength sum considerations (Baur, 1970) since, as discussed below, the latter O atoms are bonded to a tetrahedrally coordinated Zn atom rather than a third Mg atom. However, the differences are not large enough to significantly alter the systematic variation in valence angle with degree of edge-sharing: the ranges of O—Mg—O angles subtended by occupied–occupied, *occupied–vacant, and unshared octahedron edges are* 81·6 to 84·7°, 89·5 to 92·2°, and 90·5 to 100·3° respectively. Note that for all five Mg atoms, the direction of maximum thermal vibration is oriented at angles of between 5 and 13° to the *b* axis, that is towards the octahedron faces with maximum area (Table 2).*

The mean distance between the centre of the vacant octahedron (at 0·227, 0·0, 0·909) and its surrounding O atoms is 2·207 Å. This value is significantly larger

* See previous footnote.

(by 0·125 Å) than the average Mg–O bond length in the occupied octahedra, but can be readily understood in terms of the relatively larger electrostatic repulsion between O atoms in the absence of a central cation.

In the past it has been the practice to discuss edge-length and valence-angle distortions associated with the sharing of edges (or faces) between coordination polyhedra qualitatively in terms of the competition between cation–cation and anion–anion Coulombic repulsive interactions along and across the shared polyhedral elements (Pauling, 1960; Baur, 1972). However, recent semi-empirical molecular-orbital studies of shared-edge distortions in a number of structures, including silica–W (Tossell & Gibbs, 1976), olivine (McLarnan, Hill & Gibbs, 1979), and andalusite (Hill, Gibbs & Peterson, 1979), and various layer compounds (Peterson, Hill & Gibbs, 1978), have shown that molecular-orbital theory is capable of providing quantitative insight into the forces that determine shared-edge configurations in solids. In particular, calculations undertaken by Peterson *et al.* (1978) on models of the octahedral sheets in brucite display an energy minimum at a shared-edge length of 2·79 Å and a layer thickness of 2·12 Å. These values are very similar to the observed values for brucite (2·787 and 2·112 Å respectively) and, if the vacant octahedral site is ignored, are only slightly larger than the corresponding parameters for mooreite (2·758 and 2·045 Å). Indeed, had the molecular-orbital calculations been performed with an Mg–O bond length of 2·082 Å (the mean value for mooreite) rather than 2·10 Å (the brucite value) the agreement would have been closer still.

The zinc tetrahedra

The single vacant octahedral site per repeat unit in the Mg octahedron layer shares its upper and lower faces with two nonequivalent $Zn(OH)_4$ tetrahedra (Fig. 1). The Zn···Zn separation across the vacant site (3·526 Å) is at the upper end of the range of cation separations (3·02 to 3·58 Å) observed between *corner*-sharing ZnO_4 tetrahedra (Hill, in preparation). It may therefore be concluded that the increased thickness of the octahedron layer in this region is more a function of the absence of shared octahedron edges in the layer itself, rather than of the presence of strong Zn···Zn repulsive interactions across the sheet. Indeed, the Zn tetrahedra have suffered relatively little distortion in articulating to the octahedron layer: the maximum variation in Zn–O bond lengths is only 0·035 Å (Table 3) and the range of O–Zn–O valence angles (102 to 117°) is quite typical for Zn in this coordination. Nevertheless, the mean area of the bases of the two tetrahedra (9·05 Å^2) is significantly larger than the average area of the upper and lower faces of the occupied octahedra in the sheet (8·17 Å^2), and it is clear that articulation is dependent on the larger octahedron size achievable in the absence of a central Mg atom.

As noted in the previous section, the O–H bonds associated with the octahedron sheets are oriented perpendicular to the layers. In detail, however, this is strictly true only for the hydroxyl groups in the brucite-like portions of the sheet, that is those shared between three Mg atoms (Figs. 1 and 2): the six hydroxyl groups shared between two Mg atoms and a Zn atom on the periphery of the vacant octahedral site are, in fact, oriented at angles of between 26 and 37° to the sheet normal. In all cases the direction of tilt is away from the associated Zn atom, as expected, thereby lending credence to the proton positions determined during least-squares refinement. The fourth hydroxyl group in each Zn tetrahedron, O(5) and O(6), forms a similar angle (of about 103°) with the Zn–O bond perpendicular to the sheets, but in this case the detailed proton position is dependent on the orientation of the connecting bond to the Mn atom in the interlayer region (Fig. 2): for both of these hydroxyl groups the O atom can be assumed to be in a state of sp^2 hybridization with Zn–O–Mn bridging angles of 124 and 129°.

The manganese octahedron

The Mn atom is located almost exactly halfway between the Mg octahedron sheets and is surrounded by two hydroxyl groups (with a *cis* relationship) and four water molecules in an approximately octahedral configuration (Figs. 1 and 3). The OH groups are shared with Zn tetrahedra on opposite sides of adjacent sheets but the water molecules are anchored only by hydrogen bonds to neighbouring octahedra and sulphate groups (Table 4). Note that all four H_2O groups are oriented so as to direct their lone-pair electrons, rather than their protons, towards the layers of H atoms on the periphery of the Mg octahedron sheets (Fig. 1), and in so doing each becomes the receptor of a rather weak hydrogen bond. Aside from these interactions, the only linkage between the sheets is provided by the corner-sharing between Zn tetrahedra and Mn octahedra, thereby accounting for the perfect {010} cleavage and platy habit exhibited by the mineral.

Not surprisingly, the octahedron is oriented with two of its faces parallel to the (010) layers, but, unlike the Mg octahedra, it has suffered only a small degree of flattening (0·08 Å), consistent with the absence of shared edges. Bond lengths and angles within the polyhedron are, however, considerably distorted: the Mn–OH bond lengths of 2·106 and 2·118 Å are significantly shorter than those to the water molecules (2·217–2·307 Å), probably reflecting the smaller sum of electrostatic bond strengths received by the hydroxyl groups, while the valence angles range from 79 to 99°.

The sulphate tetrahedron

The sulphate group occupies a rather large cavity between the Mn octahedra in the interlayer region and serves to neutralize the excess positive charge resulting from the presence of the Zn^{2+} ions attached to the brucite layers. In this sense the group fulfils a similar role to the SO_4^{2-}, CO_3^{2-} and Cl^- radicals incorporated within the structures of the sodalite and cancrinite mineral groups, although the detailed environment is, of course, different in each case. Furthermore, it is unlikely that the site is underpopulated to any significant degree since the chemical analysis and the charge-neutrality constraint both limit the unit-cell content of S to an integral value (Hill, 1979).

Since the group is held in position only by several rather weak hydrogen bonds from adjacent water molecules and hydroxyl groups (Figs. 1 and 3), the 'thermal-vibration' ellipsoids, especially those of the O atoms, are quite large. Indeed, for all O atoms the directions of maximum vibration are perpendicular to the S—O bonds (Fig. 3 and Table 2). Therefore, although no attempt was made to refine the radical as a rigid group, it appears to be undergoing rotational rather than positional disorder within the cavity. Partly because of the large thermal parameters, but no doubt also as a result of the fact that the O atoms are all significantly underbonded, the S—O bond lengths are all at the lower end of the range of values observed for insular sulphate groups (Louisnathan, Hill & Gibbs, 1977). The spread of O—S—O valence angles (107 to 113°) is, however, well within the limits usually observed.

Hydrogen bonding

The distance and angle parameters describing the 13 hydroxyl groups and 4 water molecules in the asymmetric unit, along with their associated hydrogen bonds ($H\cdots O_a < 2{\cdot}5$ Å), are given in Table 4. Although there is a considerable spread among the individual O—H distances (0·48–1·03 Å), the mean value for all 21 bonds (0·73 Å) is, as normally observed, about 0·2 Å shorter than the corresponding average distance measured in other crystalline hydroxides and hydrates by neutron diffraction (Ferraris & Franchini-Angela, 1972). Similar shifts of the apparent H-atom position toward the atom to which it is bonded have been documented in a large number of structures and are generally ascribed to the relatively large distortion of electron density which takes place during formation of the O—H bond (Coppens, 1974). For this reason the $H—O_d—H$ bond angles (where O_d represents the donor O atom) are also imprecisely determined in X-ray diffraction studies, although, despite this fact, three of the four angles in mooreite are within one e.s.d. of the mean value (108°) documented by Ferraris & Franchini-Angela (1972).

With the sum of electrostatic bond strengths (Brown & Wu, 1976) as an indicator of the likelihood of a particular O atom being involved in hydrogen bonding, it is apparent that only the four sulphate O atoms, together with O(5) and O(6), are sufficiently underbonded to behave as acceptors. Of the fifteen hydrogen bonds listed in Table 4 for which the $H\cdots O_a$ distance (where O_a is the acceptor atom) is less than 2·5 Å, eleven are indeed associated with these six O atoms, while the remainder involve each of the four water molecules bonded to Mn. The distances $O_d\cdots O_a$ and angles $O_d—H\cdots O_a$ are all within the ranges of values observed in other compounds but none of the interactions can be considered to be strong, since $O_d\cdots O_a > 2{\cdot}7$ Å.

Ten of the fifteen hydrogen bonds are directed between atoms in the interlayer region (dashed lines in Fig. 3) with eight of these involving the sulphate O atoms, and two involving the H_2O and OH groups of adjacent Mn octahedra. Only five bonds are directed between OH groups in the Mg octahedron sheets and O atoms in the interlayer region. From the classification scheme of Ferraris & Franchini-Angela (1972) all four water molecules may therefore be assigned to Class 2, Type *H*, with one lone pair directed toward a divalent cation and the other toward a proton.

Cation ordering

As discussed in the structure determination section above, the population parameters of the cations were released during least-squares refinement in a crude attempt to account for possible cation disorder over these sites. The site occupancies obtained (Table 1) indicate that only 5 to 12% of the octahedral Mg and Mn atoms are disordered and that the tetrahedral Zn sites are not involved to any significant degree. This result is consistent with the chemical analysis (Hill, 1979) in the sense that the ratio Mg:Zn:Mn is observed to be close to the value 4·5:2:1 suggested from the structural analysis, and is also consistent with the fact that the mean polyhedron bond lengths are close to the values expected for chemically pure sites (Shannon, 1976). Furthermore, the two Mg sites displaying the greatest amount of (Mn) substitution are not only those with slightly larger bond lengths, but are also the two sites which share only four, rather than five, edges with neighbouring octahedra.

It is a pleasure to acknowledge the support of a Queen Elizabeth II Fellowship for the duration of this study. I am especially grateful to Dr B. M. Gatehouse of the Chemistry Department at Monash University for permission to use the PW 1100 diffractometer, and to Dr G. D. Fallon for his able assistance during data collection and processing. Calculations were performed on the CSIRO Cyber 76 and Monash Burroughs 6700

computers. Mrs S. Foster is kindly thanked for typing the manuscript.

References

ALEXANDER, L. E. & SMITH, G. S. (1964). *Acta Cryst.* **17**, 1195–1201.

ALLMANN, R. (1968). *Z. Kristallogr.* **126**, 417–426.

AMINOFF, G. (1921). *Z. Kristallogr.* **56**, 506–509.

BAUER, L. H. & BERMAN, H. (1929). *Am. Mineral.* **14**, 165–172.

BAUR, W. H. (1970). *Trans. Am. Crystallogr. Assoc.* **6**, 129–155.

BAUR, W. H. (1972). *Am. Mineral.* **57**, 709–731.

BROWN, I. D. & WU, K. K. (1976). *Acta Cryst.* B**32**, 1957–1959.

COPPENS, P. (1974). *Acta Cryst.* B**30**, 255–261.

FERRARIS, G. & FRANCHINI-ANGELA, M. (1972). *Acta Cryst.* B**28**, 3572–3583.

FINNEY, J. J. (1969). *Am. Mineral.* **54**, 973–975.

GHOSE, S. (1964). *Acta Cryst.* **17**, 1051–1057.

HILL, R. J. (1979). *Aust. Mineral.* No. 26, pp. 126–128.

HILL, R. J., GIBBS, G. V. & PETERSON, R. C. (1979). *Aust. J. Chem.* **32**, 231–241.

HORNSTRA, J. & STUBBE, B. (1972). PW 1100 data-processing program. Philips Research Laboratories, Eindhoven, Holland.

International Tables for X-ray Crystallography (1974). Vol. IV. Birmingham: Kynoch Press.

LARSON, A. C. (1967). *Acta Cryst.* **23**, 664–665.

LOUISNATHAN, S. J., HILL, R. J. & GIBBS, G. V. (1977). *Phys. Chem. Miner.* **1**, 53–69.

MCLARNAN, T. J., HILL, R. J. & GIBBS, G. V. (1979). *Aust. J. Chem.* **32**, 949–959.

PAULING, L. (1960). *The Nature of the Chemical Bond*, 3rd ed. Ithaca: Cornell Univ. Press.

PETERSON, R. C., HILL, R. J. & GIBBS, G. V. (1978). *Geol. Soc. Am. Abstr. Program*, **10**, 471.

PREWITT-HOPKINS, J. (1949). *Am. Mineral.* **34**, 589–595.

SHANNON, R. D. (1976). *Acta Cryst.* A**32**, 751–767.

SHELDRICK, G. M. (1976). *SHELX* 76. Program for crystal structure determination. Univ. of Cambridge, England.

STAHLIN, W. & OSWALD, H. R. (1970). *Acta Cryst.* B**26**, 860–863.

STEWART, J. M. (1976). Editor. The XRAY system – version of 1976. Tech. Rep. TR-446. Computer Science Center, Univ. of Maryland, College Park, Maryland.

STEWART, R. F., DAVIDSON, E. R. & SIMPSON, W. T. (1965). *J. Chem. Phys.* **42**, 3175–3187.

TOSSELL, J. A. & GIBBS, G. V. (1976). *J. Mol. Struct.* **35**, 273–287.

ZIGAN, F. & ROTHBAUER, R. (1967). *Neues Jahrb Mineral. Monatsh.* pp. 137–143.

Acta Cryst. (1980). B**36**, 1311–1319

The Nature of the Chemical Bonding in Boron Carbide, $B_{13}C_2$. III. Static Deformation Densities and Pictorial Representation

BY A. KIRFEL, A. GUPTA AND G. WILL

Mineralogisches Institut der Universität Bonn, Lehrstuhl für Mineralogie und Kristallographie, Poppelsdorfer Schloss, 5300 Bonn, Federal Republic of Germany

(*Received* 1 *December* 1979; *accepted* 8 *January* 1980)

Abstract

The crystal structure of rhombohedral $B_{13}C_2$ is composed of two structural units, the linear C—B—C chain and the B_{12} icosahedron distorted from ideal symmetry due to the different external bonding partners. Based on multipole expansion results, static deformation density maps have been calculated for sections of interest in both units. These static deformation density distributions are discussed in comparison to earlier published dynamic deformation density results. Three-dimensional pictorial representations of the static deformation densities and of total static densities of individual atoms as well as of structural fragments are given to complete the information obtainable from a multipole expansion refinement and to give a better insight into the chemical bonding in $B_{13}C_2$.

0567-7408/80/061311-09$01.00

Introduction

In two previous papers (Kirfel, Gupta & Will, 1979*a*,*b*), hereafter called I and II, the crystal structure of $B_{13}C_2$ has been studied in detail by least-squares refinements of X-ray diffraction data (I). These studies included a multipole expansion refinement (Hirshfeld, 1971; Harel & Hirshfeld, 1975), which yielded $R = 0{\cdot}028$ compared to $R = 0{\cdot}050$ for the conventional spherical-atom refinement. The numerical results like